Geophysical Research Letters

RESEARCH LETTER
10.1029/2020GL091777

Climate-Driven Variability in Runoff Erosion Encoded in Stream Network Geometry

Alexander Getraer[1] **and Adam C. Maloof**[1]

[1]Department of Geosciences, Princeton University, Princeton, NJ, USA

Key Points:

- Confluent streams in more humid climates are less likely to share a common slope and orientation
- The relative influence of drainage area and stream slope on erosion acts as a climate-sensitive control on slope ratio and stream profiles
- The branching angle of confluent streams varies systematically with climatic aridity in concert with slope ratio

Correspondence to:
A. Getraer,
agetraer@alumni.princeton.edu

Citation:
Getraer, A., & Maloof, A. C. (2021). Climate-driven variability in runoff erosion encoded in stream network geometry. *Geophysical Research Letters*, *48*, e2020GL091777. https://doi.org/10.1029/2020GL091777

Received 29 NOV 2020
Accepted 12 JAN 2021

Abstract Climate signatures recorded in the geometry of branching streams provide insight into climate and landscape histories on Earth and other planetary bodies. Recent findings establish that branching angles are narrower and stream profiles are straighter in more arid climates. However, these two observations have been attributed to different mechanisms. Here we demonstrate that for US watersheds the difference in slope between confluent streams increases with humidity, and streams with a greater difference in slope tend to branch at wider angles. Our observations suggest a branching angle endmember of 90° when stream slopes are most different. Using a simple model of runoff erosion, we show how this variation in relative stream slopes can be explained by a shift in streamflow accumulation across climate regimes. These findings connect previously observed climate signatures in branching angles and stream profiles, suggesting that both record the same control of aridity on surface flow.

Plain Language Summary Spatial patterns in stream networks have emerged as a promising tool for interpreting climate and landscape histories on Earth, as well as other planets and moons. Recent findings establish that in wetter environments, branching angles between confluent streams tend to be wider, and stream slopes flatten out more rapidly downstream. However, it remains unclear how these two observations are connected. Here we study watersheds across the contiguous United States, demonstrating that confluent streams tend to have a greater difference in slope in more humid climates. We show how greater differences in slope with increasing humidity link directly to wider average branching angles and downstream shallowing of slope. Variation in relative stream slopes across climates may be produced by climate-driven changes in drainage. We find that the area of a drainage basin has a stronger influence on erosion—and stream steepness—in wetter landscapes, supporting the theory that water flowing downstream accumulates less efficiently in drier landscapes. Our findings connect previously observed 'signatures' of climate in stream networks and offer a unifying view of how climate shapes the landscape.

1. Introduction

Branching stream networks shape Earth's landscape over a wide range of spatial scales (Horton, 1945; Montgomery & Dietrich, 1992; Perron et al., 2008), reflecting a complex signature of erosional and sediment transport processes (Rodriguez-Iturbe & Rinaldo, 2001). Understanding how climate influences these processes and controls the geometry of branching streams could provide a tool for remotely probing landscape evolution and historical climate change on Earth (Perron et al., 2012; Seybold et al., 2017) as well as other planets and moons with fluvial landscapes (Black et al., 2017; Grau Galofre et al., 2020; Pieri, 1980; Seybold et al., 2018; Stepinski & Stepinski, 2005).

The branching angle between confluent streams (α) is an essential characteristic of stream network geometry that records the influence of topographic slope and upstream drainage area on stream flow direction (Hooshyar et al., 2017; Horton, 1945; Howard, 1971; Pieri, 1984), and may reflect the shape of upstream basins (Yi et al., 2018). Seybold et al. (2017) identified a geometric signature of climate recorded in α: across the contiguous United States, mean α varies systematically with climatic aridity index (AI), from ~45° in arid environments to ~72° in humid environments. They theorized that this dependency reflects a change in the relative influence of different erosional processes on network growth across climates (Seybold et al., 2017).

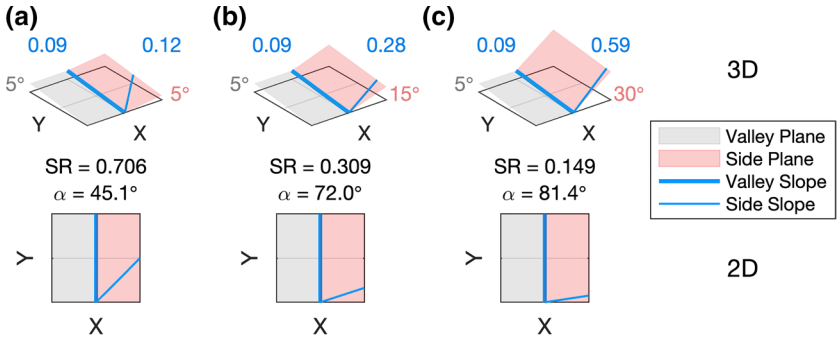

Figure 1. (a–c) In 3D view, the valley plane is inclined relative to the x-axis by the angle shown in gray, while the side plane is inclined relative to the valley plane by the angle shown in red. The steepest slopes along each plane are shown in blue and represent the expected direction of stream flow. For this simplified geometry, the angle (α) formed by the two blue "streams" in 2D is predicted exactly from SR using Equation 1. (a–c) show that as the side slope increases relative to the valley slope, the initial branching angle tends toward 90°. SR, slope ratio.

1.1. Stream Network Growth

Stream networks expand by the headward growth of drainage paths, initiated by two distinct erosional processes: channel incision by surface runoff (Horton, 1945; Montgomery & Dietrich, 1992; Perron et al., 2012) and valley head extension by diffusive groundwater flow (Devauchelle et al., 2012; Dunne, 1990). Surface runoff occurs when rainfall exceeds soil infiltration capacity, flowing downhill in the direction of steepest topographic slope and accumulating in valleys. When the shear stress along concentrated flow paths exceeds the surface's resistance to erosion, runoff erodes channels into the landscape (Dunne, 1990; Horton, 1945).

The first explanation of stream branching in a runoff-driven environment was formulated by Horton (1945). Horton observed that tributaries tend to follow the steepest slope toward a parent stream. Using a simplified geometric model of topography representing a tributary forming on the planar side-slope of a parent valley (Figure 1), he described the analytical solution for the branching angle between the tributary and parent stream. Horton's model predicts that α depends on the ratio of the parent stream's slope to that of the steeper tributary, or the slope ratio (SR):

$$\cos(\alpha) = SR \tag{1}$$

In groundwater-fed networks, groundwater, recharged by rainfall percolation to the water table, flows diffusively along subsurface pressure gradients. Seepage occurs at the termini of these flow paths, where the water table intersects the surface and discharges as a spring. Where discharge is sufficiently concentrated, seepage entrains sediment and undercuts the surface. This erosive process propagates the valley head in the direction of subsurface flow as it drains the surrounding aquifer (Dunne, 1990). Studies of known seepage networks observed a mean branching angle of 72°, matching the expected angle of bifurcating flow paths initiated in a diffusive field (Devauchelle et al., 2012; Petroff et al., 2013).

1.2. Stream Branching and Climate

In arid landscapes, local episodic precipitation typically produces ephemeral runoff and aquifers that are separated from the surface. In contrast, regular precipitation and thicker soils in humid landscapes enhance groundwater recharge, resulting in higher water tables more likely to feed surface flows (Chen et al., 2019; Seybold et al., 2017). As a result, Seybold et al. (2017) theorized that diffusive geomorphic processes such as seepage may have greater influence on branching geometry with increasing humidity, accounting for the observed widening of mean α toward 72°.

Using the analysis of Seybold et al. (2017) as a starting point, we explore additional features of stream network geometry that might extend our understanding of climate's influence on erosional process. Chen et al. (2019) showed that humid streams tend to shallow rapidly in slope downstream, while arid streams tend to have straighter profiles. They theorized that downstream flow accumulation weakens with

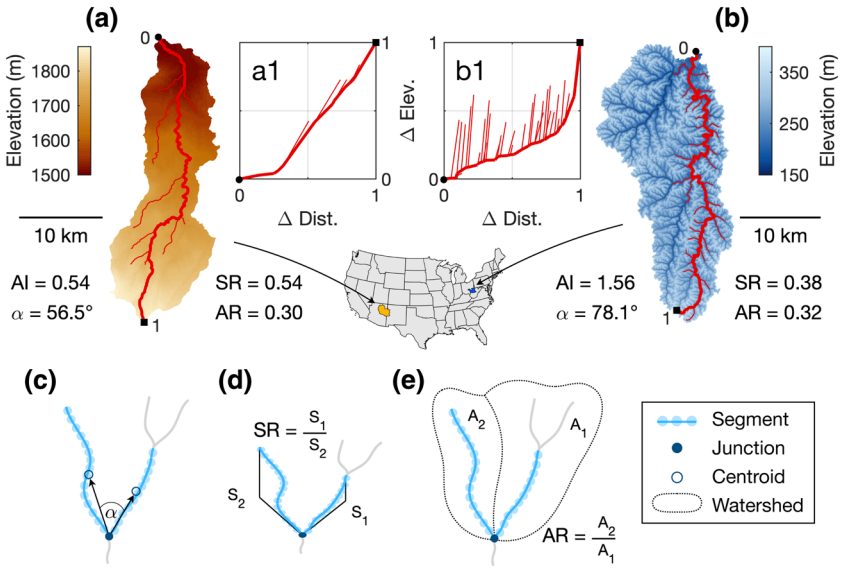

Figure 2. Representative landscapes in a drier climate (a), with mean SR > 0.5 and narrower branching angles, and (b) wetter climate, with mean SR < 0.5 and wider branching angles. Statistics for (a) and (b) come from their respective parent watersheds, Hydrologic Unit Code-6 150200 and 050302. (a1–b1) show profiles of the longest stream in each landscape and their tributary stream segments, mapped in red in (a–b), as resolved by the National Hydrography Data set. The profile of the humid landscape (b1) is more concave than that of the arid landscape (a1), producing larger differences in slope between tributary segments and the main stem. Stream segments span two junctions or a stream head and the next junction downstream. (c) α measures the difference in mean flow direction of two confluent stream segments; (d) SR measures the ratio of the shallower slope (S_1) to the steeper slope (S_2); (e) AR measures the ratio of the smaller drainage area (A_2) to the larger area (A_1). SR, slope ratio; AR, area ratio.

increasing aridity, as water tables decouple from the surface, contributing less flow and drawing more infiltration through channel beds. As a result, erosion rates in arid regimes increase less rapidly downstream, creating straighter profiles (Chen et al., 2019). Straighter profiles have more gradual changes in local elevation, implying that SR may be systematically higher across arid networks.

Horton theorized that SR predicts the branching angle of a tributary forming on an unchannelized slope, and further studies have shown that α and SR coevolve in response to changes in local relief (Howard, 1971; Pieri, 1984; Schumm, 1956). Therefore, SR may function as an initial constraint on α, and be affected by the same mechanisms underpinning the climate signature observed in α. We hypothesize that the fundamental relationship observed by Horton holds true throughout landscape evolution: as the average difference in slope between confluent streams increases, the angle at which the two streams tend to intersect increases toward 90° (Figure 1). This phenomenon should occur as a natural result of surface runoff following the steepest topographic slope.

If larger branching angles in more humid environments reflect a 72° endmember characteristic of subsurface flow, then those angles should be increasingly independent of surface slopes and display little correlation to SR. However, if stream networks in humid regimes still are dominated by runoff erosion, then a dependency between α and SR should be evident across all climates. In the latter scenario, the widening of mean branching angles with increasing humidity would be unrelated to the 72° attractor of diffusive flows. Instead, this signature would reflect that wetter landscapes have a greater proportion of stream junctions with low SR, characteristic of stream networks that shallow downstream with increasing flow (Chen et al., 2019; Whipple & Tucker, 1999).

To illustrate the idea that mean α may reflect climate sensitive distributions of SR, we use a qualitative example of two landscapes in different climate regimes. Figures 2a and 2b show digital elevation models from the arid Colorado Plateau and humid Appalachian Basin overlaid with their respective stream networks. The arid landscape with narrower α is characterized by a consistently oriented gradient and higher SR (Figure 2a), where tributaries enter the main stream in-line with a straight profile (Figure 2a1). On the other

hand, the humid landscape with wider α is characterized by greater diversity in slope orientation and lower SR (Figure 2b), where ridge-bound tributaries are increasingly out of sync with the main stream profile as the network shallows downstream (Figure 2b1). These observations imply that SR is intrinsically connected to α and profile shape, suggesting that observed climate signatures in stream network geometry may reflect systematically higher SR in more arid landscapes. To assess this hypothesis, we examine the relationships between α, SR, and climate across the United States.

2. Data and Methods

We analyzed branching streams from the publicly available ~30 m resolution National Hydrography Dataset Plus (NHDPlus) Version 2 (USEPA & USGS, 2012), mapped using the USA Contiguous Lambert Conformal Conic projection. NHDPlus includes flowline location, connectivity, drainage area, and slope magnitude for surface water features in watersheds spanning the entire contiguous United States. We first removed non-stream features and large waterbodies described by artificial centerlines, leaving 2,238,108 stream segments. These segments account for 872,664 junctions with exactly two upstream tributaries. Our analysis excludes junctions that are formed by two segments of a braided stream (24,866), have tributary slopes not resolved by the dataset (115,519), or are missing climate data (15). For each of the remaining 743,682 junctions, we calculated α, SR, the area ratio (AR), and AI (Getraer & Maloof, 2020).

2.1. Branching Geometry

We define the branching angle as the difference in mean flow direction between two confluent stream segments. Stream segments are defined by a series of connected points spanning two junctions or a stream head and the next junction, along the downstream path of a network. We measured the mean flow direction of each segment as the vector connecting a segment's centroid to its downstream junction. The angle between each pair of these vectors defines α at each junction (Figure 2c). This method discounts random fluctuations in flow direction due to meandering (similar to Seybold et al., 2017), while still accounting for the influence of local flow geometry that determines junction location (similar to Pieri, 1984).

The NHDPlus dataset assigns slope (S) and drainage area (A) values to each stream segment. S is the elevation drop along a stream segment divided by the horizontal segment length, while A is the area of the watershed upstream. We calculated SR and AR at each junction, where for two confluent streams SR is the shallower S_1 divided by the steeper S_2 (Figure 2d) and AR is the smaller A_2 divided by the larger A_1 (Figure 2e).

2.2. Aridity Index

To characterize climate across the United States, we used the aridity index AI = P/PET, where P and PET are the long-term average annual precipitation rate and potential evapotranspiration rate, respectively. PET estimates the climatic demand for water given sufficient precipitation. AI controls the partitioning of mean annual precipitation into evapotranspiration and runoff (Budyko, 1974), reflecting the availability of rainfall for plant growth and constraining regional vegetation cover (Brooks et al., 2011; Sanford & Selnick, 2013; Voepel et al., 2011). Using NHDPlus stream attribute data for P and PET from 1971 to 2000 (Wieczorek et al., 2018), we calculated mean AI at each junction. We often refer to $\log_{10}$(AI), where positive values represent increasing humidity ($P >$ PET), and negative values represent increasing aridity ($P <$ PET).

3. Results and Discussion

3.1. Branching Geometry Across Climates

We analyzed regional variation in $\log_{10}$(AI), α, and SR by averaging NHDPlus junction data across Hydrologic Unit Code-6 (HUC6) watersheds (Figure 3). After reproducing the relationship between $\log_{10}$(AI) and α first identified by Seybold et al. (2017), we found that this signal (Figure 3d) is mirrored by a previously unknown correlation between $\log_{10}$(AI) and SR (Figure 3e). Regionally, α correlates more closely with SR than with climatic aridity (Figure 3f). These new results suggest that understanding the climate sensitivity of SR is integral to interpreting observed variation in α across all climates.

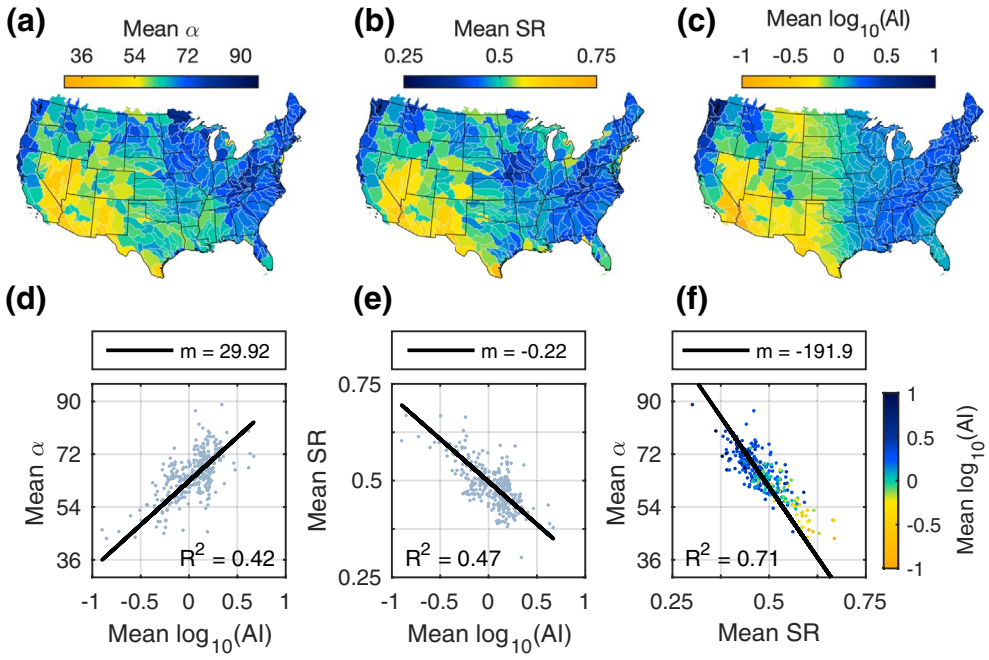

Figure 3. Mean (a) α, (b) slope ratio (SR), and (c) aridity index (AI) values for the NHDPlus dataset, regionally averaged across HUC6 watersheds for the contiguous United States. $\log_{10}$(AI) has similar explanatory power for the systematic variation observed in (d) α and (e) SR. (f) The dependence of α on SR is stronger than either variable's correlation with climatic aridity.

To explore variation in SR and α across climate regimes, we first classified the NHDPlus data into nine bins by $\log_{10}$(AI). The climate bins are equally spaced between -1 and 0.75, with the outer bins including all values below -1 and above 0.75, respectively. Figure 4a shows that the cumulative distributions of SR vary systematically with climate, such that mean SR increases as $\log_{10}$(AI) decreases. In humid climates, SR is more likely to be below 0.5, while in more arid climates, SR is more likely to be above 0.5. In subarid climates, where $-0.25 < \log_{10}(\text{AI}) < 0$, SR follows a uniform distribution, meaning that every value of SR is equally likely to be observed. Figure 4b shows that cumulative distributions of α also vary systematically with climate, such that mean α increases from 44.7° in the most arid climate to 72.1° in the most humid climate.

To understand how the systematic variation of α with $\log_{10}$(AI) observed in Figure 4b changes with SR, we categorized each climate regime distribution by SR using ten equally spaced bins from 0 to 1. Figures 4c and 4d show that across all climates, α widens toward 90° as SR decreases toward 0—the fundamental relationship observed by Horton (1945). As SR approaches 1, the dependency of α on AI emerges (Figure 4e).

The relationship between SR and α offers a new perspective on the observation that mean branching angles tend to widen with increasing humidity (Seybold et al., 2017). Splitting up the parent distributions of α by SR reveals a climate invariant endmember where $\alpha = 90°$ and SR = 0 (Figures 4c and 4d), while distributions of SR and α show that humid regimes have a greater proportion of branches approaching that endmember (Figures 4a and 4b). Even in the most extreme cases, mean SR cannot actually reach 0, and as a result, mean α inevitably falls somewhere below 90°. The finding that branching angles widen with humidity may reflect the shift in underlying SR distributions toward the 90° endmember rather than a diffusive attractor at 72°. This interpretation raises a new question: what mechanisms can account for the relatively higher abundance of branching tributaries with low SR in more humid environments?

3.2. Erosional Controls on Branching Geometry

As Figures 2a1 and 2b1 suggest, higher average SR implies more gradual changes in local elevation in arid environments, consistent with recent findings that stream profiles tend to be straighter with increasing

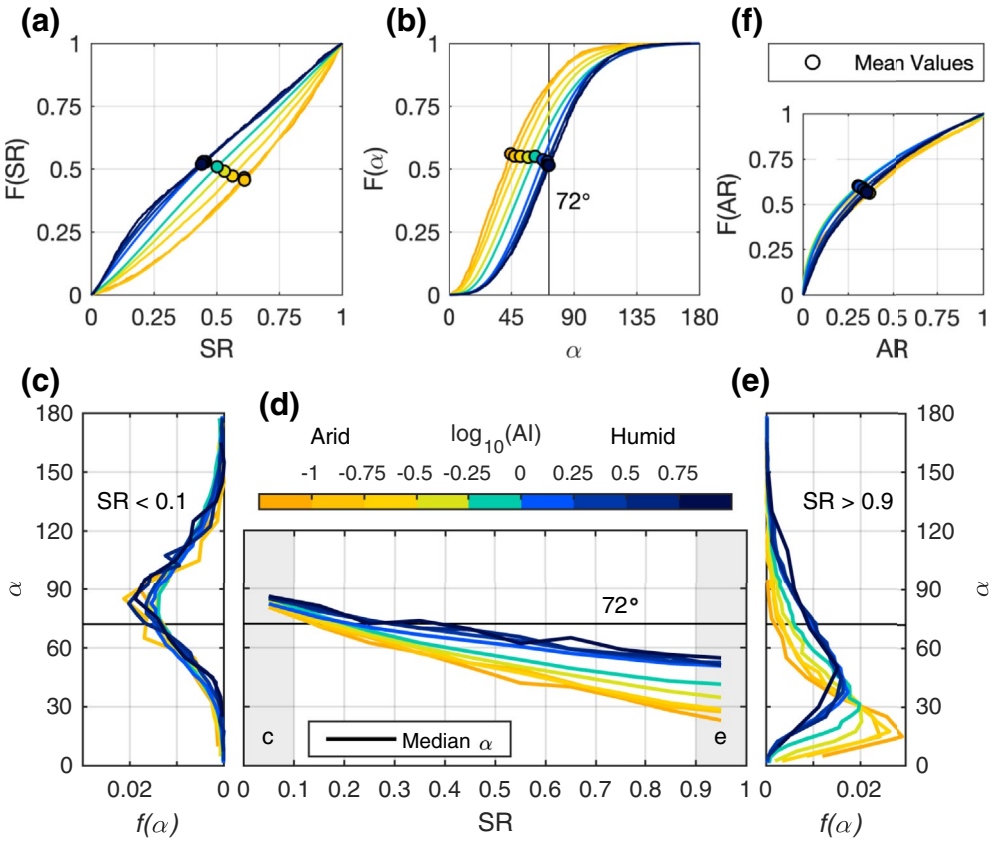

Figure 4. Distributions of (a) slope ratio (SR) and (b) α, represented by their empirical cumulative density functions, vary systematically across the nine climate regimes, with respective mean values (a) decreasing and (b) increasing as aridity index (AI) increases. (a) At the climate extremes, F(SR) appears to cluster around two "endmembers": an arid distribution with mean SR ≈ 0.61, and a humid distribution with mean SR ≈ 0.45. (b) In the most humid climates, mean α approaches 72° as the percentage of branching angles above 90° increases to ~25%. Branching angle distributions within each climate regime vary systematically across the range of SR. (c) When SR < 0.1, histograms of α peak near 90° and are fully overlapping across all climate regimes. (d) As SR increases, median α decreases and diverges by climate regime. (e) When SR > 0.9, histograms of α reflect the trend observed in Figure 4b: branching angles are narrower in more arid climates. (f) Distributions of area ratio (AR) appear insensitive to climate.

aridity (Chen et al., 2019). We describe stream profile shape using concavity (θ), which defines the scaling relationship between S and A:

$$S \propto A^{-\theta} \tag{2}$$

Profiles are concave for $\theta > 0$, straight for $\theta = 0$, and convex for $\theta < 0$. Research based on the optimization of surface runoff suggests that branching angles tend to increase with the absolute value of θ (Hooshyar et al., 2017; Howard, 1994; Pieri, 1984; Roy, 1983), but the applicability of this control across real-world networks remains unclear (Seybold et al., 2017).

Similar to Chen et al. (2019), we found that θ records a signature of AI (Figures 5a and 5b). Chen et al. (2019) hypothesized that global variation in profile shape is driven by systematic differences in downstream erosion rates, suggesting that stream flow accumulation is weaker in arid environments. Using a basic model of runoff erosion, we explore how this theory might help explain the observed variation in SR and ultimately connect to the climate sensitivity of α found by Seybold et al. (2017).

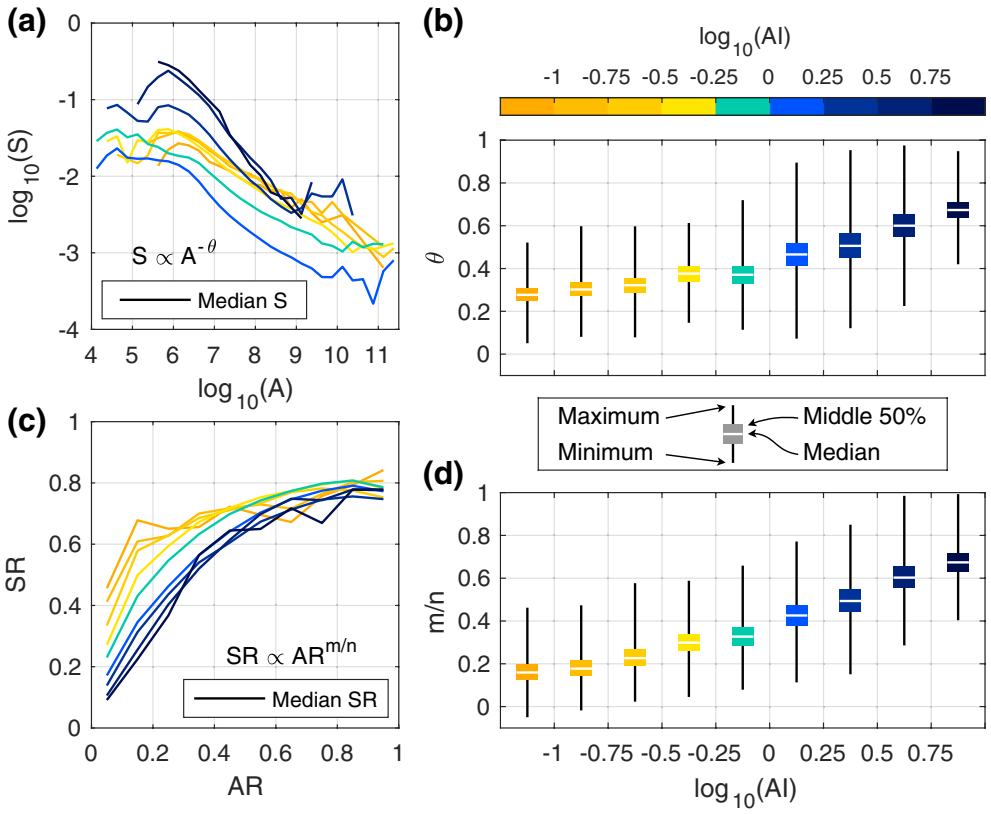

Figure 5. (a) The slope-area relationship varies with climate as (b) concavity (θ) increases with humidity. θ is influenced by the m/n ratio, which controls the relationship between slope ratio and area ratio. (c) Accordingly, the influence of AR on SR varies systematically across climate regimes. In humid environments, SR is more sensitive to AR, while in arid environments, SR remains higher with decreasing AR, as (d) m/n decreases with aridity. Distributions in (b) and (d) are created by randomly subsampling and performing linear least squares regressions on 100 junctions from each climate regime 100,000 times. SR, slope ratio; AR, area ratio.

Stream slopes are shaped by erosion and evolve to balance the long term rate of streamflow, as erosion reaches equilibrium with uplift. Erosion by surface flow $\left(-\frac{\delta z}{\delta t}\right)$ often is approximated by a power law function of drainage area (A) and stream slope (S):

$$-\frac{\delta z}{\delta t} \propto A^m S^n \tag{3}$$

where m and n reflect the nonlinear influence of drainage area and slope on erosion. A is used in place of streamflow (Q), based on the assumption that flow accumulates with drainage area according to the relationship:

$$Q \propto A^c \tag{4}$$

Assuming that confluent streams erode at the same rate, Equation 3 implies that SR scales with AR (Seidl & Dietrich, 1992) such that:

$$SR \propto AR^{m/n} \tag{5}$$

Distributions of AR appear climate invariant (Figure 4f), implying that the observed variation in SR distributions with climate (Figure 4a) is due to changes in m/n. Consistent with this hypothesis, we found that m/n is systematically lower with increasing aridity (Figures 5c and 5d).

The observed climatic variation in m/n (Figure 5d) suggests that drainage area exerts a relatively weaker influence on erosion in more arid environments, possibly reflecting diminishing flow accumulation with increasing aridity (Whipple & Tucker, 1999). Whipple and Tucker (1999) demonstrated that m/n depends on the scaling of streamflow with drainage area (Equation 4): m/n decreases with c. In humid environments, perennial flows supported by groundwater accumulate with increasing drainage area downstream. However, in arid environments, downstream accumulation is diminished due to ephemeral localized flow and loss by infiltration to decoupled water tables (Chen et al., 2019). As a result, Q is less dependent on A in arid landscapes—meaning that c, and therefore m/n, are closer to 0, as hypothesized by Chen et al. (2019) and observed in Figure 5d. When m/n is closer to 0, erosion rates change less in response to increasing A downstream. Consequently, as the difference in A between confluent streams increases, SR decreases more rapidly in humid regimes with high concavity than in arid regimes with low concavity (Figure 5c). While many processes influence stream network geometry, climate-sensitive flow accumulation emerges as a promising explanation for why SR tends to be lower with increasing humidity (Figure 4a), consistent with more concave profiles (Figures 2a1–2b1 and 5b; Chen et al., 2019) and reflected in wider α (Figure 4b; Seybold et al., 2017).

4. Conclusion

The relative influence of drainage area and stream slope on erosion—described by the m/n ratio—acts as a climate-sensitive control on stream network geometry across the contiguous United States. The control of m/n on SR distributions across climate regimes, as suggested by our results, provides a missing link between previously observed climate signatures in branching angles and profile concavity. These findings help explain overarching variation in stream network geometry, employing a holistic view of continental drainage patterns that averages over local heterogeneity to reveal the effects of climate-driven variability in runoff erosion.

Data Availability Statement

The derived multivariate dataset used to produce our results is accessible from http://hydroshare.org/resource/0b93e7c659fe4fc59bf6a202c269313c. The publicly available NHDPlus data are accessible from https://nhdplus.com/NHDPlus/ and https://doi.org/10.5066/F7765D7V.

Acknowledgments
The authors thank A. Mehra, B. Getraer, A. Irwin Wilkins, F. Simons, M. Hooshyar, B. Ferdowsi, E. Geyman, B. Howes, A. Tasistro-Hart, D. Cassidy-Nolan, reviewer J. Kirchner, and two anonymous reviewers for guidance, feedback, and insight. This research was supported by the Princeton University Department of Geosciences and Princeton Environmental Institute.

References

Black, B. A., Perron, J. T., Hemingway, D., Bailey, E., Nimmo, F., & Zebker, H. (2017). Global drainage patterns and the origins of topographic relief on Earth, Mars, and Titan. *Science*, *356*(6339), 727–731. https://doi.org/10.1126/science.aag0171

Brooks, P. D., Troch, P. A., Durcik, M., Gallo, E., & Schlegel, M. (2011). Quantifying regional scale ecosystem response to changes in precipitation: Not all rain is created equal. *Water Resources Research*, *47*(10), W00J08. https://doi.org/10.1029/2010WR009762

Budyko, M. I. (1974). *Climate and life*. New York, NY: Academic Press.

Chen, S., Michaelides, K., Grieve, S. W. D., & Singer, M. B. (2019). Aridity is expressed in river topography globally. *Nature*, *573*(7775), 573–577. https://doi.org/10.1038/s41586-019-1558-8

Devauchelle, O., Petroff, A. P., Seybold, H. F., & Rothman, D. H. (2012). Ramification of stream networks. *Proceedings of the National Academy of Sciences*, *109*(51), 20832–20836. https://doi.org/10.1073/pnas.1215218109

Dunne, T. (1990). Hydrology, mechanics, and geomorphic implications of erosion by subsurface flow. In C. Higgins, & D. Coates (Eds.), Groundwater geomorphology: The role of subsurface water in earth-surface processes and landforms, (Vol. 252, pp. 1–28). Geological Society of America. https://doi.org/10.1130/SPE252-p1

Getraer, A., & Maloof, A. C. (2020). *NHDPlus stream branching geometry and climatic aridity aggregated by junction*. HydroShare. https://doi.org/10.4211/hs.0b93e7c659fe4fc59bf6a202c269313c

Grau Galofre, A., Jellinek, A. M., & Osinski, G. R. (2020). Valley formation on early Mars by subglacial and fluvial erosion. *Nature Geoscience*, *13*(10), 663–668. https://doi.org/10.1038/s41561-020-0618-x

Hooshyar, M., Singh, A., & Wang, D. (2017). Hydrologic controls on junction angle of river networks. *Water Resources Research*, *53*(5), 4073–4083. https://doi.org/10.1002/2016WR020267

Horton, R. E. (1945). Erosional development of streams and their drainage basins; hydrophysical approach to quantitative morphology. *The Geological Society of America Bulletin*, *56*(3), 275–370. https://doi.org/10.1130/0016-7606(1945)56[275:EDOSAT]2.0.CO;2

Howard, A. D. (1971). Optimal angles of stream junction: Geometric, stability to capture, and minimum power criteria. *Water Resources Research*, *7*(4), 863–873. https://doi.org/10.1029/WR007i004p00863

Howard, A. D. (1994). A detachment-limited model of drainage basin evolution. *Water Resources Research*, *30*(7), 2261–2285. https://doi.org/10.1029/94WR00757

Montgomery, D. R., & Dietrich, W. E. (1992). Channel initiation and the problem of landscape scale. *Science*, *255*(5046), 826–830. https://doi.org/10.1126/science.255.5046.826

Perron, J. T., Kirchner, J. W., & Dietrich, W. E. (2008). Spectral signatures of characteristic spatial scales and nonfractal structure in landscapes. *Journal of Geophysical Research*, *113*(F4), F04003. https://doi.org/10.1029/2007JF000866

Perron, J. T., Richardson, P. W., Ferrier, K. L., & Lapotre, M. (2012). The root of branching river networks. *Nature*, *492*(7427), 100–103. https://doi.org/10.1038/nature11672

Petroff, A. P., Devauchelle, O., Seybold, H., & Rothman, D. H. (2013). Bifurcation dynamics of natural drainage networks. *Philosophical Transactions of the Royal Society A: Mathematical, Physical & Engineering Sciences*, *371*(2004), 20120365. https://doi.org/10.1098/rsta.2012.0365

Pieri, D. C. (1980). Martian valleys: Morphology, distribution, age, and origin. *Science*, *210*(4472), 895–897. https://doi.org/10.1126/science.210.4472.895

Pieri, D. C. (1984). Junction angles in drainage networks. *Journal of Geophysical Research*, *89*(B8), 6878–6884. https://doi.org/10.1029/JB089iB08p06878

Rodriguez-Iturbe, I., & Rinaldo, A. (2001). *Fractal river basins: Chance and self-organization*. Cambridge, UK: Cambridge University Press.

Roy, A. G. (1983). Optimal angular geometry models of river branching. *Geographical Analysis*, *15*(2), 87–96. https://doi.org/10.1111/j.1538-4632.1983.tb00771.x

Sanford, W. E., & Selnick, D. L. (2013). Estimation of evapotranspiration across the conterminous united states using a regression with climate and land-cover data. *Journal of the American Water Resources Association*, *49*(1), 217–230. https://doi.org/10.1111/jawr.12010

Schumm, S. A. (1956). Evolution of drainage systems and slopes in badlands at Perth Amboy, New Jersey. *The Geological Society of America Bulletin*, *67*(5), 597–646. https://doi.org/10.1130/0016-7606(1956)67[597:EODSAS]2.0.CO;2

Seidl, M., & Dietrich, W. (1992). The problem of channel erosion into bedrock. *Catena Supplement*, *23*(24), 101–124.

Seybold, H., Kite, E., & Kirchner, J. W. (2018). Branching geometry of valley networks on Mars and Earth and its implications for early Martian climate. *Science Advances*, *4*(6), aar6692. https://doi.org/10.1126/sciadv.aar6692

Seybold, H., Rothman, D. H., & Kirchner, J. W. (2017). Climate's watermark in the geometry of stream networks. *Geophysical Research Letters*, *44*(5), 2272–2280. https://doi.org/10.1002/2016GL072089

Stepinski, T. F., & Stepinski, A. P. (2005). Morphology of drainage basins as an indicator of climate on early Mars. *Journal of Geophysical Research*, *110*(E12), E12S12. https://doi.org/10.1029/2005JE002448

USEPA, & USGS. (2012). *National hydrography dataset Plus version 2.1*. U.S. Geological Survey. Retrieved from https://nhdplus.com/NHDPlus/

Voepel, H., Ruddell, B., Schumer, R., Troch, P. A., Brooks, P. D., Neal, A., et al. (2011). Quantifying the role of climate and landscape characteristics on hydrologic partitioning and vegetation response. *Water Resources Research*, *47*(10), W00J09. https://doi.org/10.1029/2010WR009944

Whipple, K. X., & Tucker, G. E. (1999). Dynamics of the stream-power river incision model: Implications for height limits of mountain ranges, landscape response timescales, and research needs. *Journal of Geophysical Research*, *104*(B8), 17661–17674. https://doi.org/10.1029/1999JB900120

Wieczorek, M., Jackson, S., & Schwarz, G. (2018). *Select attributes for NHDPlus version 2.1 reach catchments and modified network routed upstream watersheds for the conterminous United States*. US Geological Survey. https://doi.org/10.5066/F7765D7V

Yi, R. S., Arredondo, Á., Stansifer, E., Seybold, H., & Rothman, D. H. (2018). Shapes of river networks. *Proceedings of the Royal Society A: Mathematical, Physical & Engineering Sciences*, *474*(2215), 20180081. https://doi.org/10.1098/rspa.2018.0081